Biotechnology Journal
www.biotechnology-journal.com

Biotechnol. J. 2016, 11, 780–787

DOI 10.1002/biot.201500540

Research Article

Graphene oxide surface blocking agents can increase the DNA biosensor sensitivity

Biwu Liu, Po-Jung J. Huang, Erin Y. Kelly and Juewen Liu

Department of Chemistry, Waterloo Institute for Nanotechnology, University of Waterloo, Waterloo, Ontario, Canada

Graphene oxide adsorbs single-stranded fluorescent probe DNA, and the adsorbed probe can be desorbed by adding the complementary target DNA. Using this method, many biosensor studies have been carried out. We recently proposed a two-step mechanism for this sensing reaction: non-specific probe displacement followed by hybridization in the solution. Only about one out of six added target DNA is hybridized with the adsorbed probe to generate a signal, leading to relatively low sensitivity. In this work, we aim to test whether surface blocking agents can minimize non-specific target adsorption and increase hybridization efficiency. Over ten blocking agents (polymers, surfactants, and DNA) were screened based on their effect on probe DNA adsorption and target DNA induced probe desorption. DNA oligonucleotides show significant and controllable enhancement in sensor sensitivity. The effect of DNA length and sequence was systematically investigated. Under optimized conditions, the sensor sensitivity was enhanced by nearly 10-fold. Using the same blocking method, sensitivity enhancement of other targets was also achieved, including adenosine and Hg^{2+} with DNA aptamer probes. This reported surface blocking strategy can generally improve graphene oxide and potentially other surface adsorption based biosensors for metal ions, small molecules, and DNA.

Received	17 SEP 2015
Revised	13 NOV 2015
Accepted	14 JAN 2016
Accepted artcile online	15 JAN 2016

Supporting information available online

Keywords: Adsorption · Aptamers · Hybridization efficiency · Non-specific target adsorption · Surface blocking

1 Introduction

DNA is a very versatile molecule for developing biosensors [1–5]. In addition to simple nucleic acid targets, DNA aptamers recognize a broad range of analytes. At the same time, DNA also interacts with various nanoscale materials in a predictable and controllable manner [6–9]. A recent example is the adsorption of DNA by graphene oxide (GO) [10, 11]. Two properties make GO a very popular material for designing DNA-based biosensors. First, single-stranded DNAs (ssDNAs) are quickly adsorbed by GO [12, 13]. In the presence of a complementary DNA (cDNA), the adsorbed probe can be released from the GO surface. Second, GO is an efficient fluorescence quencher, and the release of fluorescently labeled probes is accompanied with fluorescence enhancement. Since its first report in 2009 [11], this method has been employed to design a diverse range of biosensors [14–28].

While many applied studies have been carried out, our understanding on its surface science is far from complete. We reason that such understandings may lead to further improved biosensors. For example, we recently performed a quantitative study on this system and found that the utilization of the target DNA is far from ideal [29]. For every six target DNA molecules added, only one probe DNA was desorbed. The rest of the target DNAs were adsorbed by the GO surface. This was attributed to that the affinity between DNA and GO is higher than that for DNA duplex formation. Ideally, each target DNA should produce a hybridization event. Since only less than 20% of the target DNA is used to generate a signal, there is a large room for improvement.

Correspondence: Prof. Juewen Liu, Department of Chemistry, Waterloo Institute for Nanotechnology, 200 University Avenue West, N2L 3G1, Waterloo, Ontario, Canada
Email: liujw@uwaterloo.ca

Abbreviations: cDNA, complementary DNA; **CTAB**, hexadecyltrimethyl ammonium bromide; **FAM**, 6-carboxyfluorescein; **GO**, graphene oxide; HEPES, 4-(2-hydroxyethyl) piperazine-1-ethanesulfonate; **PAA**, polyacrylic acid; **PAH**, poly(allylamine hydrochloride); **PEG**, polyethylene glycol; **PSS**, poly(styrenesulfonate); **PVS**, poly(vinylsulfonic acid, sodium salt); **SDS**, sodium dodecyl sulfate; **ssDNAs**, single stranded DNAs

Unlike many other nanomaterials, the surface of GO is special in terms of its heterogeneity [30, 31], containing highly oxidized regions with low DNA adsorption affinity, crystalline carbon regions with high affinity, and regions between these two extremes. This heterogeneity is reflected from the thermal desorption profile of DNA, where only a fraction of DNA is desorbed by heating to nearly the boiling temperature [29], while the rest are tightly adsorbed. For the fraction that desorbs, the temperature profile is very broad [13, 32]. If target DNA molecules are adsorbed on the high affinity regions, it is very difficult for them to generate a signal. Therefore, one rational way to improve the sensor performance is to block the GO surface, especially the high affinity binding sites.

Surface blocking is a common practice in biosensor development. Well-known examples include blocking gold surfaces with thiolated compounds and blocking nitrocellulose with bovine serum albumin (BSA). Due to its heterogeneous nature, blocking the GO surface might require a more subtle control of surface forces. If a blocking agent is too strong, probe adsorption might be affected, leading to weak signal. If too weak, the intended blocking effect might not be achieved. Since many types of molecules can be adsorbed by GO and serve as potential blocking agents, a systematic comparison is needed to maximize the performance of DNA sensing. In this work, we screened over ten blocking agents. Under optimized conditions, we significantly improved the signaling sensitivity of a few targets including a DNA, a small molecule and a metal ion.

2 Materials and methods

2.1 Chemicals

All DNA samples were purchased from Integrated DNA Technologies, Inc. (Coralville, IA). Sequences and modification of DNA are shown in Supporting information, Table S1. The GO sample was from Advanced Chemical Supplier (ACS) Material (Medford, MA). Polyethylene glycol (PEG, MW 20 000) was purchased from VWR. Tween 20 was from Amresco. Other polymers – polyacrylic acid (PAA, MW 15 000), poly(allylamine hydrochloride) (PAH, MW 17 000), poly(styrenesulfonate) (PSS, MW 70 000), poly(vinylsulfonic acid, sodium salt) (PVS) – and surfactants – sodium dodecyl sulfate (SDS), hexadecyltrimethyl ammonium bromide (CTAB) were purchased from Sigma. Adenosine, sodium chloride, magnesium chloride, mercury perchlorate, and 4-(2-hydroxyethyl) piperazine-1-ethanesulfonate (HEPES) were purchased from Mandel Scientific (Guelph, Canada). Milli-Q water was used in all experiments.

2.2 Quenching efficiency measurement

The GO/blocker conjugate was prepared by mixing GO (final concentration 100 μg/mL) with various blockers (polymers, surfactants, DNA) in buffer A (5 mM HEPES, 100 mM NaCl, and 10 mM $MgCl_2$). After 1 h incubation at room temperature, 10 μL of the GO/blocker mixture was added into 90 μL of the same buffer consisting of the FAM 24-mer DNA (20 nM, 50 nM, or 100 nM) in a 96-well plate. The final concentrations of surfactants (CTAB, Tween and SDS) and polymers (PEG, PAH, PAA, PSS and PVS) were 0.1% and the A_{15} DNA was 100 nM. The fluorescence intensity of the FAM 24-mer DNA was monitored using a microplate reader (Tecan Infinite F200Pro).

2.3 Kinetics of probe DNA desorption by cDNA

The DNA/GO/blocker complex with varying concentrations of blocker was prepared as mentioned above. Desorption experiment was carried out with the microplate reader. Each well contained 90 μL of buffer A and 10 μL of a DNA/GO/blocker complex solution. cDNA was then added to initiate the desorption reaction. The final concentrations of FAM 24-mer and cDNA were 50 nM and 20 nM, respectively. To investigate the effect of DNA length, DNA homopolymers A_n (n-mer DNA composed of adenine, n = 5, 7, 10, 15, and 30) with the same total adenine base concentration were used. Therefore, the final concentrations of these DNAs were 150 nM (A_5), 110 nM (A_7), 75 nM (A_{10}), 50 nM (A_{15}), and 25 nM (A_{30}), respectively. To test the effect of DNA sequence, four types of 15-mer DNA homopolymers (50 nM) were used (i.e. A_{15}, T_{15}, C_{15}, and G_{15}). In the dual fluorophore-labeled DNA experiment, 50 nM AF-A_{15} (Alexa 647 labeled A_{15}) was pre-adsorbed onto GO (10 μg/mL). After the further adsorption of the FAM 24-mer DNA (10 nM), cDNA was added (20 nM) into the solution. The emissions at the two channels were recorded (FAM: excitation at 485 nm, emission at 535 nm; AF: excitation at 612 nm, emission at 670 nm) by the plate reader.

2.4 Temperature-dependent desorption

GO (100 μg/mL) was first incubated with A_{15} (500 nM) in HEPES buffer (5 mM, pH 7.6) containing NaCl 100 mM, $MgCl_2$ 2 mM for 1 h. FAM 24-mer DNA was then added to the solution with final concentration of 500 nM. After another 1 h incubation, 5 μL of the conjugate solution was dispersed in 45 μL of HEPES buffer (50 mM, pH 7.6) in a polymerase chain reaction (PCR) tube. FAM 24-mer/GO conjugate with the same concentrations in the absence of A_{15} was also prepared. The fluorescence as a function of temperature was monitored by a real-time PCR thermocycler (CFX-96, BioRad).

2.5 Sensitivity measurement

The FAM 24-mer/GO conjugate and aptamer/GO conjugate in buffer A were prepared using the method above. Varying concentrations of targets (cDNA, Hg^{2+}, or aden-

osine) were introduced into the solution. After 1 h incubation, the fluorescence was scanned. The concentrations of the probes in FAM 24-mer/GO, Hg^{2+}-apt/GO, ade-apt/GO were 20 nM, 50 nM, and 50 nM, respectively. The concentration of the surface blocker A_{15} in Hg^{2+} or adenosine aptamer/GO system was 50 nM.

3 Results and discussion

3.1 Blockers do not inhibit probe DNA adsorption

The sensing scheme of our study is shown in Fig. 1A, where a fluorophore-labeled DNA (called probe DNA) is adsorbed by GO to form a quenched sensing complex. The probe is desorbed in the presence of the target cDNA to increase fluorescence. In the ideal case, each target DNA should hybridize with a probe DNA to light up one fluorophore. However, our previous work indicated that it takes about six target DNAs to desorb one probe. We suspected that some probes/target DNAs are adsorbed by some high affinity regions on GO, leading to decreased hybridization efficiency. The goal here is to develop an optimal blocking agent to improve DNA hybridization efficiency (Fig. 1B). Since it is difficult to rationally predict the best blocking agent, we carried out a screening experiment. Three types of molecules were tested: (i) small molecule surfactants including anionic SDS, cationic CTAB, and non-ionic Tween 20; (ii) polymer blockers including anionic PSS, PVS, PAA, cationic PAH, and neutral PEG; and (iii) various DNA sequences (see Supporting information, Fig. S1 for their structures). We did not include proteins since they are likely to interfere with heavy metal detection and thus are not general-purpose blockers.

For the screening assay, the first criterion is that a blocking agent should not adversely affect probe DNA adsorption. By using a FAM-labeled 24-mer DNA (named FAM 24-mer, Supporting information, Table S1), DNA adsorption was followed by fluorescence quenching. Using a GO concentration of 10 g/mL, quantitative DNA adsorption was achieved when the DNA concentration was lower than 150 nM (Supporting information, Fig. S2). Therefore, we chose to test three DNA probe concentrations (20 nM, 50 nM, and 100 nM), all below the adsorption capacity. At low probe concentrations (20 nM, and 50 nM), over 95% of the fluorescence was quenched by GO regardless of the type of blocker added (Fig. 2A, black and red bars). With 100 nM probe, quantitative adsorption was still achieved in the presence of most blockers (green bars). Only three blockers (i.e. Tween 20, PEG and PSS) resulted in a lower quenching efficiency of ~80%. Note that most of the blockers (except for the DNA blockers) were added in excess (more than the capacity of DNA on GO if fully adsorbed). Therefore, the blockers do not appear to adversely affect DNA adsorption. We can also rationalize their interactions based on simple surface force considerations. For example, negatively charged PAA and PVS may not adsorb onto the negatively charged GO surface because of charge repulsion. Positively charged PAH could provide additional electrostatic attractions to bridge negatively charged DNA and GO. Tween 20, PEG and PSS may strongly bind to GO via hydrophobic interactions, and may not be displaced by the probe DNA, resulting in a lower DNA adsorption capacity. The com-

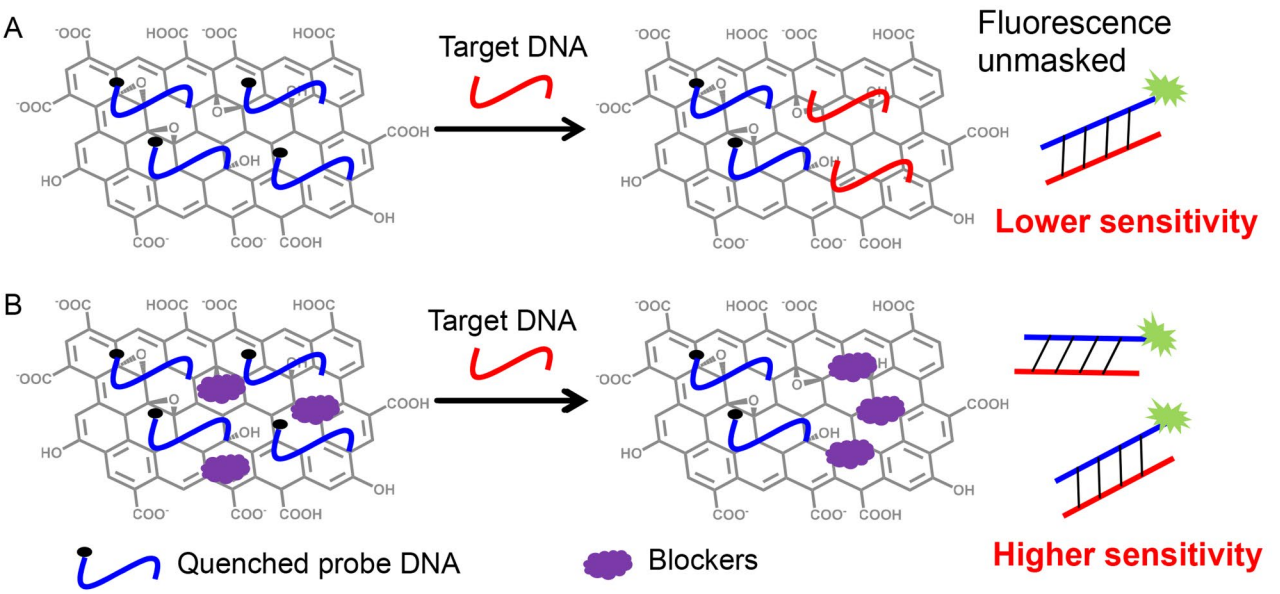

Figure 1. Schemes of GO-based sensors for target DNA sensing (**A**) in the absence and (**B**) in the presence of surface blocking agents. The fluorescence of adsorbed probe DNA is quenched, and the fluorescence is recovered in the presence of target DNA. With blocking molecules, release of the probe DNA by the target DNA is facilitated.

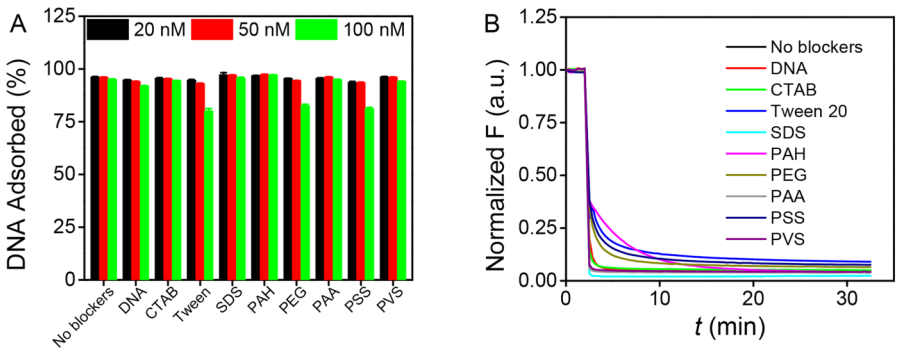

Figure 2. Effect of surface blockers on (**A**) the quenching efficiency of GO (10 μg/mL) and (**B**) adsorption kinetics using the FAM 24-mer DNA as a probe. The concentration of surfactants (CTAB, Tween and SDS) and polymers (PAH, PEG, PAA, PSS and PVS) was 0.1% and that of DNA (A15) was 100 nM. Various concentration of FAM 24-mer (20 nM, 50 nM, and 100 nM) was tested for the quenching efficiency. The adsorption kinetics were recorded using 50 nM of the FAM 24-mer DNA added at 2 min. The error bars in (**A**) represent standard deviation from three individual experiments.

plex interactions between DNA, blockers and GO are also reflected from the kinetic traces (Fig. 2B). Tween 20, PSS, and PEG slightly impeded the DNA adsorption, indicating their competitive interactions with GO. PAH also retarded DNA adsorption, which might be attributed to the electrostatic interaction with the probe DNA. Overall, the probe adsorption kinetics were still quite fast, all reached equilibrium in 10 min. In general, DNA adsorption is not significantly affected by the presence of the blockers, and all the blockers were further screened for the next step: the probe desorption reaction.

3.2 Improved DNA sensing by surface blocking

After understanding the effect of the blockers on probe adsorption, we next evaluated their effect on cDNA-induced probe desorption, which is the key step for DNA detection. To have a complete understanding, we incubated GO with each blocker of various concentrations (polymer and surfactant: 0.001, 0.01, and 0.1%; DNA [A_{15}]: 20 nM, 50 nM, and 100 nM) without further purification. After probe adsorption, the cDNA was added to induce desorption, which was monitored by fluorescence enhancement. Among the five types of polymers we tested here, neutral PEG (Fig. 3A) and negatively charged PSS (Fig. 3B) improved cDNA-induced probe desorption when the blocker concentration was as high as 0.1%. This improved signaling may be due to the blocking of high affinity regions on GO by the blocker and thus the cDNA can be more efficient in hybridizing with the target. This result is consistent with our probe DNA adsorption result (Fig. 2). On the other hand, cationic PAH (Fig. 3C) inhibited probe desorption, attributable to its additional electrostatic attractive forces between DNA (either ssDNA or dsDNA) and GO; even if a duplex were formed in the presence of cDNA, it might still adsorb by GO without fluorescence signal. The remaining two polymers, PAA (Fig. 3D) and PVS (Fig. 3E), did not exhibit a positive role in the release of the probe DNA.

We next tested the effect of surfactants, which may exert both hydrophobic and electrostatic interactions with DNA and GO. For cationic CTAB, an adverse role on the fluorescence recovery was observed when the concentration was higher than 0.01% (Fig. 3F). It is interesting to note a dramatic enhancement occurred when the CTAB concentration was 0.001%. Such an enhancement may be due to the facilitated target DNA adsorption followed by duplex formation. However, neither the probe nor the target DNA can escape from the GO surface if the CTAB concentration is too high (0.01 and 0.1%). On the other hand, the negative SDS inhibited desorption especially at high concentrations, which might be due to the highly negative surface preventing the target DNA approaching the GO surface (Fig. 3G). Lastly, the neutral surfactant Tween 20 seems to be an excellent blocker in enhancing DNA sensing (Fig. 3H). All three concentrations of Tween 20 show a similar signal recovery. Again, this is consistent with observations that Tween 20 competes with DNA adsorption on the GO surface.

The last type of blocker we tested was DNA, and a homo-polymer DNA (A_{15}) was used (Fig. 4A). Different from polymers and surfactants, the A_{15} DNA enhanced the probe DNA recovery with increased A_{15} concentration. A_{15} could strongly bind to GO through π-stacking. Such a positive correlation between the concentration of A_{15} and the signal enhancement makes the sensing process more controllable compared the other blockers. To further evaluate the role of DNA on the blocking and sensing process, we tuned the DNA length and sequence. We fixed the A base concentration and tested the effect of DNA length on the probe desorption kinetic. Longer DNA binds to GO stronger through multiple interaction sites. The strong interaction impeded probe adsorption, which is indicated by the increasing background with increasing DNA length in Fig. 4B. For example, only ~90 % of the fluorescence was quenched in the presence of A_{30}. For all these samples, the amount of fluorescence enhancement was higher with the blocker DNAs than without.

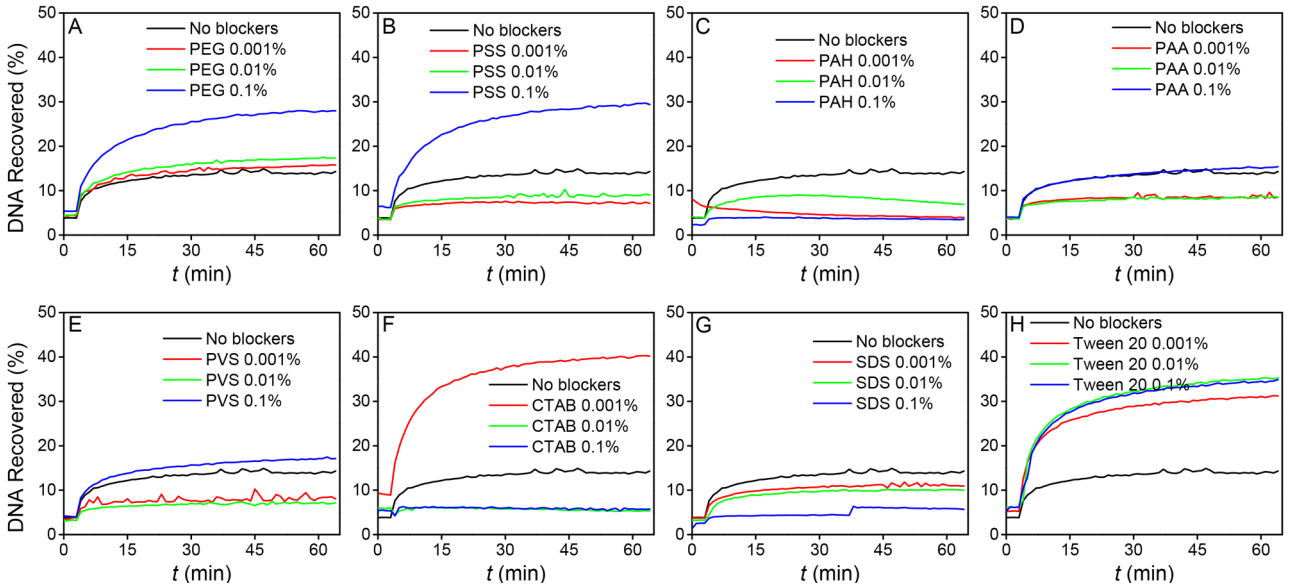

Figure 3. Probe desorption kinetics induced bycDNA in the presence of (**A**) PEG, (**B**) PSS, (**C**) PAH, (**D**) PAA, (**E**) PVS, (**F**)CTAB, (**G**) SDS, and (**H**) Tween 20. The final concentrations of polymers or surfactants were 0.001, 0.01, and 0.1% w/w. FAM 24-mer (50 nM)/GO (10 μg/mL) conjugates were prepared in buffer A in the presence of various blockers. Desorption kinetics were recorded using 20 nM of the cDNA added at 2 min.

In the presence of A_{30}, almost 50% of the fluorescence was recovered. Since the concentration of the target DNA was only 40% of the adsorbed probe DNA, 40% of fluorescence recovered means that all targets were used to form duplexes. This enhancement could be due to the formation of duplex. The complete desorption of probe DNA indicates that the very high affinity sites on GO have been effectively blocked. We also compared DNA with various sequences (Fig. 4C). It has been accepted that T binds to GO weakly, and lower enhanced kinetic was observed. G_{15} has a complex secondary structure, which decreases the affinity between GO. As a result, it did not show significant enhancing ability. Overall, poly-A and poly-C DNA showed good blocking effect.

Therefore, we have identified four potential blockers (PEG, PSS, Tween 20, and A_{15}) that can accelerate the process of cDNA-induced probe recovery. From our current study, they all share the same feature of effectively competing with DNA for adsorption on GO (Supporting information, Table S2). The GO surface is heterogeneous with both hydrophobic and hydrophilic regions. Blockers bearing interaction sites with GO (hydrophobic interaction, π-π stacking) could occupy the surface and inhibit the unspecific adsorption of target DNA [33]. Negative charges in the blocker may repel incoming DNA and positive charged blocker may provide additional attractive forces. PEG could bind to the surface through either hydrophobic interactions or hydrogen bonds. PEG has proven to be an effective blocking agent for plastic surface through hydrophobic interactions and inhibits the unspecific interaction between DNA and a 96-well plate surface [34]. PSS, a negatively charged polymer, showed inhibition of desorption at low concentrations. This could be due to the presence of the benzene group in the polymer chain that provides additional attractive forces to the target. Non-charged Tween 20 could largely increase desorption efficiency even at low concentrations without the disturbance of charged headgroups on DNA. Among the few candidates that showed improved DNA sensing performance, we chose to use DNA to perform further sensitivity studies. On one hand, the DNA sequence and length could be controlled so that we can adjust the binding affinities between DNA blockers and GO. On the hand, the interaction between target DNA and GO surface involved multiple interaction forces: electrostatic interaction, π-π stacking, hydrogen bonding. Such a complex interaction can be maximally simulated by DNA itself.

To understand the mechanism of sensitivity improvement by blocking agents, we used Alexa Fluor 647 (AF) labeled DNA as blocker (AF-A_{15}). As such, the adsorption and desorption events of blocker and probe can be monitored simultaneously. After adsorption of the AF-A_{15} blocker, further addition of the probe (FAM 24-mer, 10 nM) and target (cDNA, 20 nM) only induced a small amount of displacement of the blocker (~0.7 nM and 1.5 nM, Fig. 4D, black curve). By monitoring the FAM channel, we identified that the addition of cDNA resulted in 3.1 nM DNA duplex (blue curve). As a control, in the absence of blocker (AF-A_{15}), only 0.5 nM probe DNA recovery was observed (green curve). Our previous work has reported that the first step in DNA/GO sensing process is mainly the non-specific adsorption of the target DNA. Herein, we further proved that non-

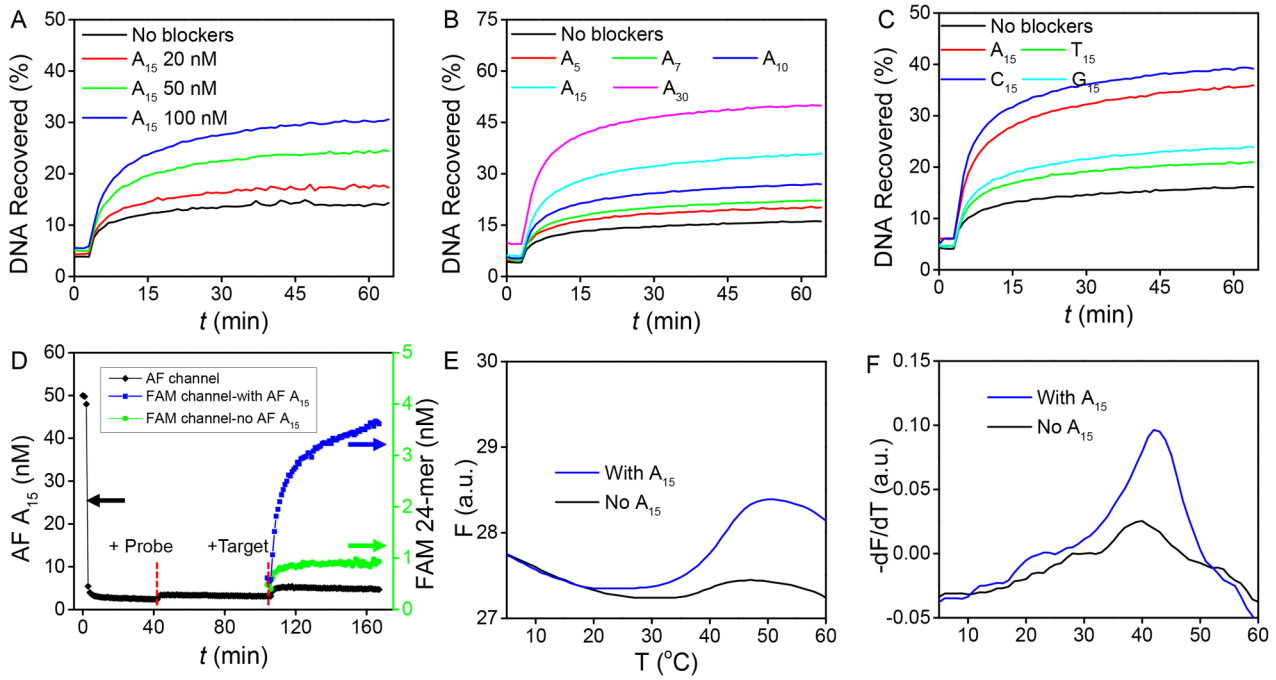

Figure 4. Homopolymer DNA as surface blockers to enhance cDNA detection. Kinetics of probe desorption as functions of (**A**) blocker concentration, (**B**) length, and (**C**) sequence. The total concentration of the base A was 750 nM in the length study. FAM 24-mer (50 nM)/GO (10 μg/mL) conjugates were prepared in buffer A in the presence of various homopolymer DNA. The cDNA (20 nM) was added at 2 min. (**D**) Kinetics of probe adsorption and target induced probe desorption in the absence and presence of AF-A15 blocking agent. FAM 24-mer DNA was used as the probe DNA. (**E**) Temperature dependent desorption kinetics of the FAM 24-mer/GO complex in the presence and absence of A15. (**F**) First derivative of the temperature dependent desorption profiles.

complementary DNA (AF-A_{15} here) on the GO surface could block such non-specific interaction and increase the efficiency of probe-target hybridization. Also, we tested the stability of the DNA-GO conjugates as a function of temperature (Fig. 4E and 4F). The FAM 24-mer/GO did not show obvious desorption at the buffer condition (50 mM HEPES, 10 mM NaCl, 0.2 mM $MgCl_2$) (Fig. 4E, black curve). The presence of a blocker (A_{15}) resulted in more probe desorption at the same condition (blue curve). The difference in the thermal stability suggested that more FAM 24-mer DNA probe adsorbed to the weak sites of GO surface due to the pre-adsorbed A_{15}, which blocks incoming DNA from adsorbing onto high affinity sites.

3.3 Improved biosensor sensitivity for DNA, adenosine, and Hg^{2+} detection

To evaluate if such signal enhancement can be used for improving sensor performance, we then measured the sensor sensitivity using the DNA/GO conjugate in the presence of A_{15} blocker. The signal recovery toward a certain concentration of target is dependent on the probe concentration (Supporting information, Fig. S3). While a high concentration of probe can maximize the duplex formation, it also increases the sensor background and an additional washing step is required [29]. Here, we used a low concentration of FAM 24-mer as probe (20 nM) and no washing or purification process was carried out. As shown in Fig. 5A, when the target concentration was lower than 5 nM, no significant fluorescence signal was observed in the absence of the blocker (Fig. 5A, black squares). However, in the presence of A_{15}, even 2.5 nM cDNA induced an observable signal change. To quantify the role of A_{15} as a blocker, we calculated the slope of the linear response range (Supporting information, Table S3). The slope in the presence of A_{15} (100 nM) was 10-fold more than that in the absence of A_{15}. In the sensor field, the sensor sensitivity is defined as the slope of the calibration curve. Therefore, the A_{15} blocker increased the sensitivity by 10-fold. It needs to be noted that we previously used a high probe concentration to fully cover the GO surface. Even under that condition, only one out of six added target DNA was used for probe hybridization [29]. In this current work, we used a lower probe concentration. Without the blocker, the usage of the target DNA was even less efficient. Therefore, with the blocker, we could improve the sensitivity by 10-fold.

Next we aimed to test whether the enhancement is also applicable to aptamer-target sensing systems (Fig. 5B and 5C). For this purpose, we adsorbed FAM-labeled adenosine and Hg^{2+} aptamers on GO, respectively. In both cases, improved signaling sensitivity

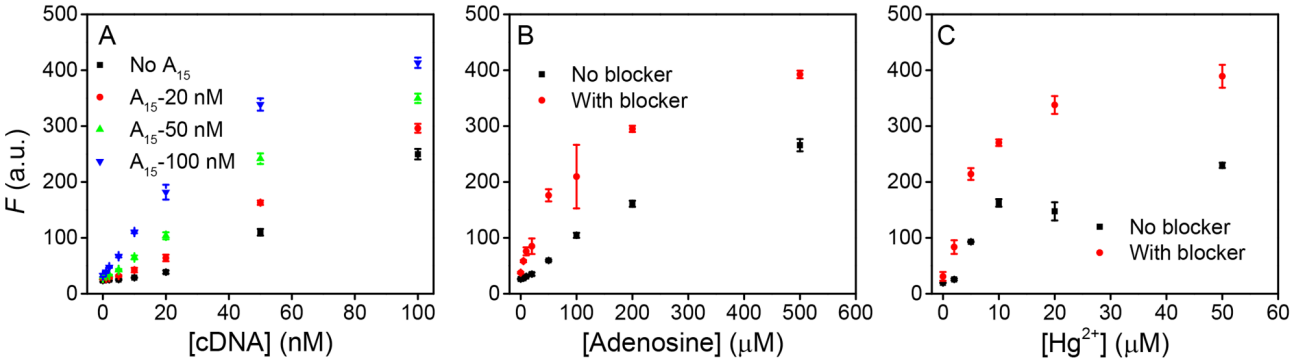

Figure 5. Effect of blocker (A15) on the performance of different sensing platforms: (**A**) cDNA detection, (**B**) adenosine detection, and (**C**) Hg^{2+} detection. DNA/GO conjugates by incubating FAM 24-mer DNA, FAM ade-apt, or FAM Hg^{2+}-apt with GO in buffer A with or without the blocker. The concentration of the surface blocker (A15) was 50 nM in adenosine and Hg2+ detection. Error bars represent standard deviation from three individual experiments.

was indeed observed. Adenosine could bind to the GO surface via π-π stacking, hydrogen bonding. The incorporation of A_{15}, which has more binding sites, largely reduced the non-specific interaction between adenosine and GO. As a result, the probe recovered by 5 μM adenosine in the presence of the blocker is comparable to that by 50 μM in the absence of the blocker. Hg^{2+} is unlikely to displace the probe DNA into solution. We reason that the increased sensitivity is probably attributed to the fact that the blocker DNA adsorbed more on high affinity regions on GO. The probe DNA, therefore, adsorbs on low affinity regions on GO. The weakly adsorbed probes can more easily react with Hg^{2+} to induce desorption. In particular, the Hg^{2+} aptamer is rich in thymine, which has low affinity towards the GO surface.

4 Concluding remarks

In summary, we screened various surface blocking agents to increase sensitivity of the DNA/GO biosensor system. This work was inspired by our previous work on the mechanism of DNA/GO sensing process, where only a small fraction of the target DNA was used for probe hybridization, and the rest was adsorbed by the GO surface. The blocking agents occupied the GO surface through π-π stacking, hydrophobic interactions or hydrogen bonding so that non-specific adsorption of targets on the GO surface can be greatly reduced. Also, the probe DNA is adsorbed on the low affinity regions on GO. As a result, the sensor sensitivity was improved.

Funding for this work is from The Natural Sciences and Engineering Research Council of Canada (NSERC).

The authors declare no financial or commercial conflict of interest.

5 References

[1] Willner, I., Zayats, M., Electronic aptamer-based sensors. *Angew. Chem. Int. Ed.* 2007, *46*, 6408–6418.
[2] Zhao, W., Brook, M. A., Li, Y., Design of gold nanoparticle-based colorimetric biosensing assays. *ChemBioChem* 2008, *9*, 2363–2371.
[3] Li, D., Song, S., Fan, C., Target-responsive structural switching for nucleic acid-based sensors. *Acc. Chem. Res.* 2010, *43*, 631–641.
[4] Fang, X., Tan, W., Aptamers generated from cell-SELEX for molecular medicine: A chemical biology approach. *Acc. Chem. Res.* 2010, *43*, 48–57.
[5] Liu, J., Cao, Z., Lu, Y., Functional nucleic acid sensors. *Chem. Rev.* 2009, *109*, 1948–1998.
[6] Wang, H., Yang, R., Yang, L., Tan, W., Nucleic acid conjugated nanomaterials for enhanced molecular recognition. *ACS Nano* 2009, *3*, 2451–2460.
[7] Katz, E., Willner, I., Integrated nanoparticle–biomolecule hybrid systems: Synthesis, properties, and applications. *Angew. Chem. Int. Ed.* 2004, *43*, 6042–6108.
[8] Liu, J., Adsorption of DNA onto gold nanoparticles and graphene oxide: Surface science and applications. *Phys. Chem. Chem. Phys.* 2012, *14*, 10485–10496.
[9] Rosi, N. L., Mirkin, C. A., Nanostructures in biodiagnostics. *Chem. Rev.* 2005, *105*, 1547–1562.
[10] He, S. J., Song, B., Li, D., Zhu, C. F. et al., A graphene nanoprobe for rapid, sensitive, and multicolor fluorescent DNA analysis. *Adv. Funct. Mater.* 2010, *20*, 453–459.
[11] Lu, C.-H., Yang, H.-H., Zhu, C.-L., Chen, X. et al., A graphene platform for sensing biomolecules. *Angew. Chem. Int. Ed.* 2009, *48*, 4785–4787.
[12] Tang, Z. W., Wu, H., Cort, J. R., Buchko, G. W. et al., Constraint of DNA on functionalized graphene improves its biostability and specificity. *Small* 2010, *6*, 1205–1209.
[13] Wu, M., Kempaiah, R., Huang, P.-J. J., Maheshwari, V. et al., Adsorption and desorption of DNA on graphene oxide studied by fluorescently labeled oligonucleotides. *Langmuir* 2011, *27*, 2731–2738.
[14] Chen, D., Feng, H., Li, J., Graphene oxide: Preparation, functionalization, and electrochemical applications. *Chem. Rev.* 2012, *112*, 6027–6053.
[15] Wang, Y., Li, Z., Hu, D., Lin, C.-T. et al., Aptamer/graphene oxide nanocomplex for in situ molecular probing in living cells. *J. Am. Chem. Soc.* 2010, *132*, 9274–9276.
[16] Pei, H., Li, J., Lv, M., Wang, J. et al., A graphene-based sensor array for high-precision and adaptive target identification with ensemble aptamers. *J. Am. Chem. Soc.* 2012, *134*, 13843–13849.

[17] Zhang, H., Jia, S., Lv, M., Shi, J. et al., Size-dependent programming of the dynamic range of graphene oxide–DNA interaction-based ion sensors. *Anal. Chem.* 2014, *86*, 4047–4051.
[18] Wang, Q., Xu, N., Gui, Z., Lei, J. et al., Catalytic activity of a dual-hemin labelled oligonucleotide: Conformational dependence and fluorescent DNA sensing. *Chem. Commun.* 2014, *50*, 15362–15365.
[19] Chang, H., Tang, L., Wang, Y., Jiang, J. et al., Graphene fluorescence resonance energy transfer aptasensor for the thrombin detection. *Anal. Chem.* 2010, *82*, 2341–2346.
[20] Zhang, M., Ye, B.-C., A reversible fluorescent DNA logic gate based on graphene oxide and its application for iodide sensing. *Chem. Commun.* 2012, *48*, 3647–3649.
[21] Tang, Q., Zhang, Q., Jiang, Y., Li, J. et al., Competitive assembly to increase the performance of the DNA/carbon-nanomaterial-based sensing platform. *ACS Appl. Mater. Interfaces* 2014, *6*, 13470–13477.
[22] Lin, Y., Tao, Y., Pu, F., Ren, J. et al., Combination of graphene oxide and thiol-activated DNA metallization for sensitive fluorescence turn-on detection of cysteine and their use for logic gate operations. *Adv. Funct. Mater.* 2011, *21*, 4565–4572.
[23] Park, J. S., Goo, N.-I., Kim, D.-E., Mechanism of DNA adsorption and desorption on graphene oxide. *Langmuir* 2014, *30*, 12587–12595.
[24] Liu, M., Song, J., Shuang, S., Dong, C. et al., A graphene-based biosensing platform based on the release of DNA probes and rolling circle amplification. *ACS Nano* 2014, *8*, 5564–5573.
[25] Li, H., Li, W., Nie, Z., Yao, S., A label-free and time-resolved luminescence strategy for the detection of proteins based on DNA-Tb^{3+} luminescence quenched by graphene oxide. *Analyst* 2015, *140*, 6386–6391.
[26] Tang, L., Wang, Y., Li, J., The graphene/nucleic acid nanobiointerface. *Chem. Soc. Rev.* 2015, *44*, 6954–6980.
[27] Deng, R., Tang, L., Tian, Q., Wang, Y. et al., Toehold-initiated rolling circle amplification for visualizing individual microRNAs in situ in single cells. *Angew. Chem. Int. Ed.* 2014, *53*, 2389–2393.
[28] Wang, Y., Tang, L., Li, Z., Lin, Y. et al., In situ simultaneous monitoring of ATP and GTP using a graphene oxide nanosheet–based sensing platform in living cells. *Nat. Protoc.* 2014, *9*, 1944–1955.
[29] Liu, B., Sun, Z., Zhang, X., Liu, J., Mechanisms of DNA sensing on graphene oxide. *Anal. Chem.* 2013, *85*, 7987–7993.
[30] Gómez-Navarro, C., Meyer, J. C., Sundaram, R. S., Chuvilin, A. et al., Atomic structure of reduced graphene oxide. *Nano Lett.* 2010, *10*, 1144–1148.
[31] Erickson, K., Erni, R., Lee, Z., Alem, N. et al., Determination of the local chemical structure of graphene oxide and reduced graphene oxide. *Adv. Mater.* 2010, *22*, 4467–4472.
[32] Huang, P.-J. J., Liu, J., A molecular beacon lighting up on graphene oxide. *Anal. Chem.* 2012, *84*, 4192–4198.
[33] Lu, C.-H., Li, J., Lin, M.-H., Wang, Y.-W. et al., Amplified aptamer-based assay through catalytic recycling of the analyte. *Angew. Chem. Int. Ed.* 2010, *122*, 8632–8635.
[34] Liu, B., Huang, P.-J. J., Zhang, X., Wang, F. et al., Parts-per-million of polyethylene glycol as a non-interfering blocking agent for homogeneous biosensor development. *Anal. Chem.* 2013, *85*, 10045–10050.

Cover illustration

This special issue, in collaboration with the Asian Federation of Biotechnology and edited by Professors Eiichi Tamiya and Chunhai Fan, covers advances in biosensors. This issue includes articles on optimization of biosensors for better sensitivity, exploration of the graphene interface for DNA analysis, aptamers for developing biosensors, etc. Image: © kentoh – Fotolia.com

Biotechnology Journal – list of articles published in the June 2016 issue.

Research Article

Quantification of total phosphorothioate in bacterial DNA by a bromoimane-based fluorescence method

Lu Xiao and Yu Xiang

http://dx.doi.org/10.1002/biot.201500432

Biotech Method

Label-free optical detection of C-reactive protein by nanoimprint lithography-based 2D-photonic crystal film

Tatsuro Endo, Hiroshi Kajita, Yukio Kawaguchi, Terumasa Kosaka and Toshiyuki Himi

http://dx.doi.org/10.1002/biot.201500440

Biotech Method

Imaging of enzyme activity using bio-LSI system enables simultaneous immunosensing of different analytes in multiple specimens

Toshiki Hokuto, Tomoyuki Yasukawa, Ryota Kunikata, Atsushi Suda, Kumi Y. Inoue, Kosuke Ino, Tomokazu Matsue and Fumio Mizutani

http://dx.doi.org/10.1002/biot.201500559

Rapid Communication

Aptamer-aptamer linkage based aptasensor for highly enhanced detection of small molecules

Van-Thuan Nguyen, Bang Hyun Lee, Sang Hoon Kim and Man Bock Gu

http://dx.doi.org/10.1002/biot.201500433